Magnetic domains of single-crystal $Nd_2Fe_{14}B$ imaged by unmodified scanning electron microscopy

Cite as: Journal of Applied Physics **83**, 6843 (1998); https://doi.org/10.1063/1.367664
Published Online: 13 October 1998

L. H. Lewis, J.-Y. Wang and P. Canfield

Magnetic domains of single-crystal $Nd_2Fe_{14}B$ imaged by unmodified scanning electron microscopy

L. H. Lewis and J.-Y. Wang[a)]
Department of Applied Science, Brookhaven National Laboratory, Upton, New York 11973-5000

P. Canfield
Ames Laboratory and Department of Physics and Astronomy, Iowa State University, Ames, Iowa 50011

The stray flux manifestations of surface magnetic domains found in as-grown $Nd_2Fe_{14}B$ single crystals were observed, with a resolution in the range of 1 μm, using conventional scanning electron microscopy (SEM) without instrumental modifications. A modified image-distortion mode was applied to image the three-dimensional stray flux emanating from the sample. The simplicity of the technique and the ready adaptability of the SEM to such modifications as *in situ* current and magnetic field application suggest that the results of this study may be extended to investigations of other materials of technological interest, such as perpendicular media disks. © *1998 American Institute of Physics.* [S0021-8979(98)30411-9]

INTRODUCTION

The magnetic domain structure of magnetically ordered materials provides information of both fundamental and applied technological interest. Data concerning the micromagnetic state, the influence of inhomogeneities on the position of domain walls, and direct determinations of the domain size and behavior under dynamical conditions are useful for the determination of materials parameters as well as for the confirmation of modeling predictions. On the more practical side, magnetic domain imaging can be used as a quick way to ascertain the presence, character, and effects of defects in recording media, recording heads, and transformer alloys.

Magnetic domain images may be generated by a variety of techniques, each with its particular strengths and drawbacks.[1] Scanning electron microscopy (SEM) allows magnetic domains of bulk materials to be imaged by the deflection of a beam of incident electrons from the surface of a ferromagnetic material under the influence of $\mathbf{F}_{\text{Lorentz}}$. In this work, the applicability of SEM for imaging magnetic domains is demonstrated on a single-crystal specimen of $Nd_2Fe_{14}B$. It is hoped that a demonstration of the relative ease of this technique, combined with the adaptability of the SEM to such modifications as external field and current application as well as environment and temperature control, may prove to be helpful for researchers in both academia and industry.

EXPERIMENTAL DETAILS

Single crystals with the composition $Nd_2Fe_{14}B$ were grown out of a Nd-rich melt from high-purity elements placed in a tantalum crucible and cooled at $\sim 1\,^{\circ}$C/h from 1190 to 800 °C. After cooling, well-formed prismatic crystals were removed from the excess flux. Room-temperature demagnetization curves indicate that the crystal possesses a coercivity under 1 Oe.

The magnetic domain observation was performed on a JEOL Model 6400 scanning electron microscope using a LaB_6 filament operated at 6 kV and 9 nA. The collector bias voltage was set at the factory to vary with the accelerating voltage, thus producing a high signal-to-noise ratio. The scanning electron microscope has not been modified or augmented in any way. Depending upon the domain characteristics of the material under investigation, either the type I or the type II contrast mode is available in SEM to image magnetic domains.[2] Type I contrast is applicable when the emitted secondary electrons possess a relatively low kinetic energy (<10 eV) sensitive to deflection by the stray field emanating from the surface of the magnetic material. Type I contrast is operative on high anisotropy, uniaxial materials with surface stray fields unconfined by closure domains to remain within the material, which are characteristics of $Nd_2Fe_{14}B$. These surface stray fields reside above alternate domain walls and exert Lorentz forces $\mathbf{F}_{\text{Lorentz}}$ on the secondary electrons which are deflected in opposite directions, depending upon the polarity of the stray field. Magnetic contrast is produced when an unequal flux of secondary electrons reach the detector, positioned at an angle to the sample's surface. In this manner the intensity of domain contrast varies from a maximum to a minimum across a single domain.[3,4] The domain contrast obtained by SEM is highly influenced by the surface morphology, because secondary electrons also give rise to a topographical image. In order to insure that the crystal surfaces were as smooth as possible, the specimen was mounted in a Gatan dual ion mill on a special sample holder to accommodate its thickness. The specimen surfaces were first ultrasonically cleaned in acetone and then ion milled in an Ar^+ beam for a total of 6 h at 3 kV and 0.5 mA. Metallic luster, in addition to a significant increase in the clarity of the domain images, was then obtained after this treatment. Experiments were conducted with the samples in the ''as-is'' condition except for the surface cleaning procedure described above. The initial working distance of the microscope was set at 39 mm, where it is ex-

[a)]Present address: Applied Materials, 3050 Bowers Ave., Santa Clara, CA 95054; electronic mail: lhlewis@bnk.gov

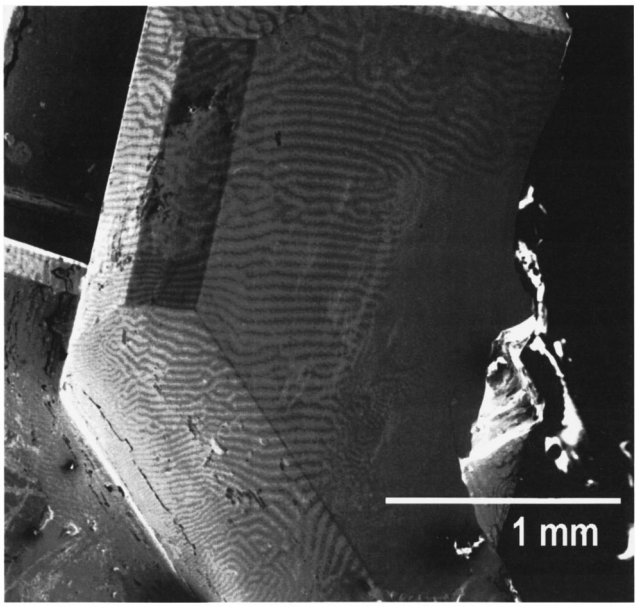

FIG. 1. Macroscopic view of the domain configuration on the (001) surface of the $Nd_2Fe_{14}B$ crystal.

pected that the external field from the objective lens would have little effect on the sample.[5] Optical Kerr microscopy was also performed on same crystal at Rhône-Poulenc Inc. for image comparison.

RESULTS AND DISCUSSION

Figure 1 presents the familiar maze pattern of domains visible on the (001) plane of the $Nd_2Fe_{14}B$ single crystal. No change of the macroscopic domain structure of the $Nd_2Fe_{14}B$ crystal was observed with change in focusing strength, even at the shortest working distance allowed by the system (8 mm). Thus the magnetic field, due to objective lens, experienced by the sample is less than the coercivity of the crystal (1 G). Higher magnifications of the maze pattern reveal a fine structure which appears to consist of strings of neutral-grey beads separated by light and dark undulating lines. Figure 2(a) shows the magnetic domain images formed by electrons influenced by the Lorentz force $+\mathbf{F}_{\text{Lorentz}}$. Features on the order of 1 μm may be resolved. Each ''bead'' in the string is elliptical in shape, with the eccentricity increasing from round on the (100) surface to more elongated on other surfaces. The depth-of-field of the secondary electron imaging process produces a third dimension, causing the strings of beads to appear either concave-up or concave-down in alternate rows. By rotating the sample through an angle of 180° a change in the contrast is produced, because the Lorentz force changes in sign. This phenomenon is shown in Fig. 2(b), where the circled feature which possesses a concave-up appearance in the top portion of Fig. 2(b) possesses a concave-down appearance in the bottom portion of the figure. Kerr microscopy, Fig. 2(c), confirms that imaged ''beads'' are in reality spike domains, residing in rows of alternating magnetization between the larger stripe or ''parallel plate'' domains which extend through the bulk of the material. Spike domains are expected to form on the surfaces of uniaxial magnetic crystals with very high anisotropies,

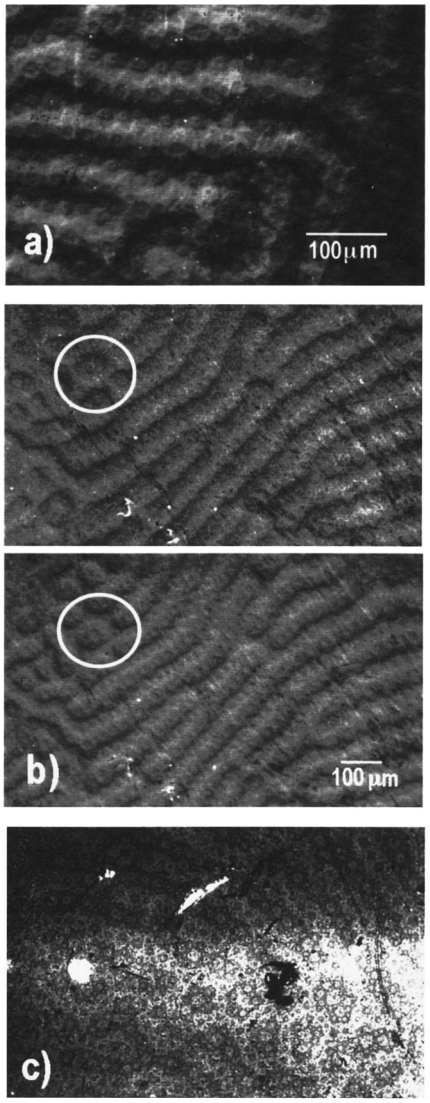

FIG. 2. (a) Higher-magnification image of the $Nd_2Fe_{14}B$ crystal, illustrating the fine structure of the domains. (b) Top: domain structures imaged at a rotation angle of 0°. Bottom: Specimen rotated by 180° relative to the original orientation. Circled regions indicate an inversion of the domain depth of field contrast. (c) Kerr micrograph of the same crystal surface imaged in (a) and (b).

such as $Nd_2Fe_{14}B$, that cannot easily form closure domains. The increased eccentricity of the spike domains found on surfaces oblique to the (001) surface may be understood as a manifestation of flux minimization for surfaces that contain only a component of the easy direction, as discussed by Goodenough.[6] No domain contrast was observed on a surface that is parallel to an easy direction, such as a $(hk0)$ surface.

A novel feature of using secondary electrons to image magnetic materials is that the demagnetizing stray fields present at the material's surface can be viewed three dimensionally, as shown in Figs. 3(a)–3(c). The (001) surface of the sample is tilted such that there is a shallow angle with respect to the optical axis of the microscope. The fringing fields appear as parallel rows of hillocks separated by narrow troughs, suggesting that the origin of the stray fields are the parallel plate/maze domains that extend through the bulk of the crystal, not the surface spike domains.

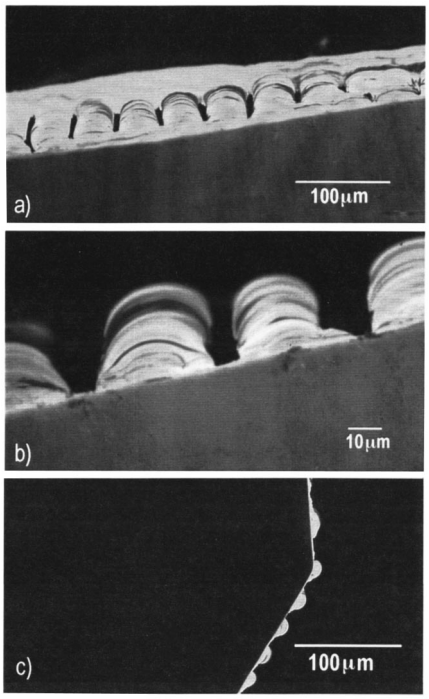

FIG. 3. (a) Image of the surface stray fields emanating from the crystal. (b) Enlargement of (a), illustrating the stray-field trough and hillock formations; (c) end-on view of surface flux from two crystallographic facets.

Generally, the image quality of magnetic contrast generated by $\mathbf{F}_{\text{Lorentz}}$ in SEM is generally poor. Both extensive theoretical[7–9] and experimental[10–12] studies have been conducted to seek optimal parameters to improve the image quality. In most cases sample surface decoration[13,14] or extensive image processing[15] is still required. Recent work by others indicated that it was necessary to externally alter the detection system of the secondary electrons; Szmaja[15] introduced an aperture in front of the secondary electron collector to act as an energy selector. Instead of having such an attachment inside the specimen chamber, the JEOL 6400 SEM is equipped, at the factory, with an automated bias adjustment circuitry to the collector which itself then acts as an energy filter. It should be borne in mind that this technique is most suitable for materials with a large, perpendicular magnetization vector because the resolution of the image is proportional to the Lorentz force of the excitation volume, as well as inversely proportional to the working distance between the detector and the specimen. However, materials with smaller magnetizations relative to $Nd_2Fe_{14}B$ may be imaged, with comparable resolution, using a smaller electron accelerating voltage.

A high density of reversed spike domains are observed on all surfaces except the easy-plane (110) surface, with a resolution on the order of 1 μm. This technique may prove to be useful for a quick and relatively simple characterization of a magnetic material surface condition and domain structure. It has the additional advantage over other magnetic domain imaging techniques in that a large area of material may be examined at one time. The simplicity of the technique and the ready adaptability of the SEM to such modifications as *in situ* current and magnetic field application may allow direct simulations and observations of a magnetic material operational performance.

ACKNOWLEDGMENTS

The authors thank Professor R. Gambino, Dr. W. McCallum, and Dr. B.-M. Ma of Rhône-Poulenc Inc. for helpful discussions and assistance. Research was performed under the auspices of the U.S. Department of Energy, Division of Materials Sciences, Office of Basic Energy Sciences under Contract No. DE-AC02-76CH0001. Ames Laboratory is operated by Iowa State University for the Department of Energy under Contract No. W-7405-ENG-82.

[1] M. R. Scheinfein, J. Unguris, D. T. Piece, and R. J. Celotta, J. Appl. Phys. **67**, 5932 (1990).
[2] J. P. Jakubovics, *Magnetism and Magnetic Materials*, 2nd ed. (University Press, Cambridge, 1994).
[3] D. C. Joy and J. P. Jakubovics, Br. J. Appl. Phys. Ser. 2 **2**, 1367 (1969).
[4] T. Yamamoto and K. Tsuno, Phys. Status Solidi A **28**, 479 (1975).
[5] A. Gopinth, *Quantitative Scanning Electron Microscopy*, edited by D. B. Holt (Academic, New York, 1974).
[6] J. B. Goodenough, Phys. Rev. **102**, 356 (1956).
[7] D. J. Fathers, J. P. Jakubovics, D. C. Joy, D. E. Newbury, and H. Yakowitz, Phys. Status Solidi A **20**, 535 (1973).
[8] G. A. Jones, Phys. Status Solidi A **36**, 647 (1976).
[9] O. C. Wells, J. Microsc. **144**, RP-1 (1986).
[10] G. W. Kammlott, J. Appl. Phys. **42**, 5156 (1971).
[11] D. J. Fathers, J. P. Jakubovics, D. C. Joy, D. E. Newbury, and H. Yakowitz, Phys. Status Solidi A **22**, 609 (1974).
[12] J. Fidler, H. Kirchmayr, and P. Skalicky, Philos. Mag. **35**, 1125 (1977).
[13] R. Gemperle, V. Kambersky, J. Simsova, L. Murtinová, L. Pust, P. Gomert, W. Schuppel, and R. Gerber, J. Magn. Magn. Mater. **118**, 295 (1993).
[14] R. Gemperle, L. Murtinová, and V. Kambersky, Phys. Status Solidi A **158**, 229 (1996).
[15] W. Szmaja, J. Magn. Magn. Mater. **153**, 215 (1996).

Published without author corrections